Recessive Mutations in *COL25A1* Are a Cause of Congenital Cranial Dysinnervation Disorder

Jameela M.A. Shinwari,[1] Arif Khan,[1,2] Salma Awad,[3,6] Zakia Shinwari,[4,6] Ayodele Alaiya,[4] Mohamad Alanazi,[5] Asma Tahir,[1] Coralie Poizat,[3] and Nada Al Tassan[1,*]

Abnormal ocular motility is a common clinical feature in congenital cranial dysinnervation disorder (CCDD). To date, eight genes related to neuronal development have been associated with different CCDD phenotypes. By using linkage analysis, candidate gene screening, and exome sequencing, we identified three mutations in collagen, type XXV, alpha 1 (*COL25A1*) in individuals with autosomal-recessive inheritance of CCDD ophthalmic phenotypes. These mutations affected either stability or levels of the protein. We further detected altered levels of sAPP (neuronal protein involved in axon guidance and synaptogenesis) and TUBB3 (encoded by *TUBB3*, which is mutated in CFEOM3) as a result of null mutations in *COL25A1*. Our data suggest that lack of COL25A1 might interfere with molecular pathways involved in oculomotor neuron development, leading to CCDD phenotypes.

Congenital cranial dysinnervation disorders (CCDDs) are a heterogeneous group of neurogenic syndromes of the ocular muscle and facial innervation; the mutated genes influence brainstem and cranial nerve development.[1] Most CCDDs present with abnormal ocular motility; these include congenital fibrosis of the extraocular muscles type 1, 2, and 3 (CFEOM1 [MIM 135700], CFEOM2 [MIM 602078], and CFEOM3 [MIM 600638]), HOXA1 spectrum (MIM 142955), horizontal gaze palsy with progressive scoliosis (HGPPS [MIM 607313]), Duane retraction syndrome (DRS [MIM 126800]), and Moebius syndrome (MBS [MIM 157900]).[2–7]

Mutations in different genes contribute to CCDD etiology by affecting neuronal development. Expressions of certain genes influence the development of the cranial nerves through molecular events including the cytoskeleton microtubule dynamics and axon path guidance. In CFEOM1, dominant mutations in *KIF21A* (MIM 608283) alter the kinesin microtubule-associated protein that normally inhibits microtubule growth inside the cell and directs axon growth toward the oculomotor muscles.[3] There is probably a recessive cause for CFEOM1 that is yet to be determined.[8] Complete loss of the oculomotor nerves for both eyes occur in CFEOM2, where homozygous mutations in the homeodomain transcription factor (*PHOX2A* [MIM 602753]) affect the survival of the oculomotor and trochlear motor neurons during development.[9] Retinal dysfunction is also part of the CFEOM2 phenotype.[10] In CFEOM3 and rarely in CFEOM1, heterozygous mutations in the cytoskeletal network gene known as neuron-specific component β-tubulin III (*TUBB3* [MIM 602661]) underlie the phenotype; the encoded protein interacts with kinesin and influences guidance of the cranial nerves.[11] Rare cases of CFEOM3 can also be caused by heterozygous mutations in *KIF21A*.[12] One of the most common CCDD phenotypes is DRS, which typically presents with lack of abduction, adduction constraint, globe retraction, and palpebral fissure narrowing on attempted adduction.[13] Although most cases of DRS are idiopathic and not familial, mutations in *CHN1* (MIM 118423) were identified in families with dominant DRS. This gene plays a role in abducens and oculomotor nerve development by controlling ocular motor axon path-finding mechanisms.[14] Homozygous mutations in *HOXA1* (MIM 142955) were identified in individuals with bilateral DRS associated with hearing and cardiovascular abnormalities,[5] and mutations in *ROBO3* (MIM 608630), which encodes an axon guidance molecule, lead to autosomal-recessive HGPPS.[15] Recessive mutations in *ECEL1* (MIM 605896), a gene that might play a role in neuromuscular junction formation, cause CCDD phenotypes in the setting of arthrogryposis.[10] Despite the genetic heterogeneity that might explain these variable phenotypes, mutations in common CCDD genes do not underlie common forms of incomitant strabismus.[16]

We identified a consanguineous Saudi family with four children, three of whom were affected by CCDD, congenital ptosis, or DRS. The proband (II.1) presented with right congenital ptosis covering the upper half of the pupil. His sister (II.2) had bilateral congenital ptosis covering the upper half of the pupil, and his affected brother (II.3) had no ptosis but presented with bilateral DRS (exotropic form in the right eye, esotropic form in the left eye). The fourth male sibling had a completely normal ophthalmic examination, as did both parents. DNA was extracted from parents and all affected and unaffected children after obtaining informed consent according to the institutional

[1]Department of Genetics, Research Center, King Faisal Specialist Hospital and Research Centre, P.O. Box 3354, Riyadh 11211, Saudi Arabia; [2]Division of Pediatric Ophthalmology, King Khaled Eye Specialist Hospital, P.O. Box 7191, Riyadh 11462, Saudi Arabia; [3]Cardiovascular Research Program, Research Center, King Faisal Specialist Hospital and Research Centre, P.O. Box 3354, Riyadh 11211, Saudi Arabia; [4]Stem Cell and Tissue Engineering Program, Research Center, King Faisal Specialist Hospital and Research Centre, P.O. Box 3354, Riyadh 11211, Saudi Arabia; [5]Genome Research Chair, King Saud University, P.O. Box 2455, Riyadh 11451, Saudi Arabia
[6]These authors contributed equally this work
*Correspondence: naltassan@kfshrc.edu.sa
http://dx.doi.org/10.1016/j.ajhg.2014.11.006.

rules and regulations (KFSHRC RAC # 2080020, KKESH 0424-P). To determine the underlying genetic defect in this family, we first sequenced all coding exons of *KIF21A*, *PHOX2A*, *HOXA1*, *TUBB3*, and *ROBO3*. No coding or splice site pathogenic mutations were identified in these genes.

After excluding mutations in the reported candidate genes as a possible genetic cause for CCDD in this family, we proceeded with linkage analysis by Affymetrix GeneChip Human Mapping 250K. Multipoint linkage analysis assuming an autosomal-recessive mode of inheritance[17] detected a potential disease locus on chromosome 4q24–25 with a maximum logarithm of odds (LOD) score of 2.5. Candidate genes in the 5.12 Mb linkage region were prioritized with suspects software,[18] and the entire open reading frames (ORFs) for 18 of the 30 annotated genes in the region were amplified and sequenced (Table S1, Figure S1 available online). Subsequent analysis of sequencing data revealed a homozygous missense mutation in exon 21 of *COL25A1* (c.1144G>A, RefSeq accession number NM_198721.3) leading to a p.Gly382Arg substitution in the encoded protein (primers listed in Table S2). This mutation cosegregated with the phenotype in family A in an autosomal-recessive manner and was absent in 500 ethnically matched normal control subjects. Based on this finding, *COL25A1* exons were screened in 41 single CCDD case subjects; several known and unknown variants were identified in *COL25A1* including 33 intronic variants, 3 synonymous polymorphisms, and 1 nonsynonymous variant (Table S3). Only one heterozygous nonsense mutation in exon 28 (c.1489G>T) was identified in a single nonfamilial case (DRSA1) that presented with exotropic DRS. This mutation, which is predicted to result in a premature stop codon (p.Gly497Ter), was also present in his unaffected brother DRSA2. To position another disease locus in this case, representative regions of *COL25A1* promoter were sequenced and CNV analysis was conducted for both siblings via the Affymetrix GeneChip Mapping 6.0 kit. Analysis was performed with the Affymetrix Genotyping Console (v.3.01) against ethnically matched normal control subjects. No mutations were detected in the promoter region but a heterozygous CNV deletion of 12.4 kb spanning exons 4–10 of *COL25A1* (chr4: 109,852,901–109,976,457, UCSC GRCh37/hg19, Figure S2) was identified in the affected DRSA1 individual, and this CNV was absent in the unaffected sibling. The origins of the CNV deletion could not be determined because DNA from parents was unavailable for analysis.

Next we preformed whole-exome sequencing with SureSelect Human All Exon kit and Illumina HiSeq 2000 Sequencer (Illumina) on the proband from family A and the affected single case subject DRSA1. The resulting variants in the linkage region were filtered as homozygous (coding or splicing) in the identified linkage region (heterozygous in the single case) and absent in the dbSNP database (GRCh37) and 1000 Genomes database. Analysis confirmed the presence of the homozygous c.1144G>A and the heterozygous c.1489G>T mutations and the absence of other pathogenic mutations in the linkage region and in genes involved in overlapping phenotypes including previously identified DRS and hereditary congenital ptosis related loci/genes: *SALL4* (MIM 607343),[19] *CHN1*,[14] *PTOS1* (MIM 178300),[20] *ZFHX4* (MIM 606940),[21] *TUBB2B* (MIM 612850),[22] and *HOXB1* (MIM 142968).[23]

Collagen, type XXV, alpha 1 (*COL25A1*) encodes a transmembrane protein that consists of an N-terminal intracellular noncollagenous domain, a transmembrane domain, and three extracellular collagen-like domains separated by four noncollagenous domains. The collagen-like domains contain unique repetitive patterns (Gly-X-Y) that stabilize the triple helix. Proteolytic cleavage of COL25A1 by furin convertase produces a soluble form known as collagen-like amyloidogenic component (sCLAC).[24,25] sCLAC folds into a protease-resistant triple helical molecule that binds fibrillized amyloid beta (Abeta) and further assembles amyloid fibrils into protease-resistant aggregates during the fibril elongation stage.[25,26] It also binds heparin but the binding of sCLAC to Abeta is influenced by the stability of its triple helical structure and competition with heparin binding.[25] sCLAC was identified as a component of senile plaques amyloid (SPs) isolated from the brains of Alzheimer disease case subjects.[24] Amyloid beta (A4) precursor protein (APP) is cleaved predominantly (about 90%) by α secretase to release soluble protein α (sAPP α) and slightly (about 10%) by β and γ secretases to release soluble protein β (sAPP β) and Abeta peptide. The accumulation of neurotoxic Abeta peptide leads to amyloid plaque and Alzheimer disease development.[27] sCLAC plays a critical role in regulating the buildup of Abeta fibrils, and properly folded sCLAC triple helices were reported to inhibit Abeta fibril formation in vitro. Once Abeta fibrils are formed, sCLAC supports their assembly into protease-resistant aggregates.[26,28] None of our case subjects had any family history of Alzheimer-related phenotype, but this does not rule out the possibility of the disease developing later in these individuals.

We investigated the expression of *COL25A1* by using cDNA libraries from commercially available multiple human adult and fetal tissues (Genemed Synthesis and Capital Biosciences) and primers specific for *COL25A1* (Table S2). In addition, immunohistochemistry (IHC) was performed to ascertain the tissue distribution of COL25A1 in E12 and E16 mouse embryos, whole mouse eye, and human eye muscle. Anti-COL25A1 antibodies (LS-B664 LifeSpan BioSciences or H00084570-B01, Novus Biological) were used after ensuring their specificity via peptide competition assay against COL25A1 full-length recombinant protein (H00084570-P01, Novus Biological). Our cDNA analysis demonstrated that *COL25A1* is ubiquitously expressed in different adult and fetal tissues. COL25A1 was also detected in different parts of mouse embryos. When cDNA expression was further examined in differential adult human brain tissues, abundant

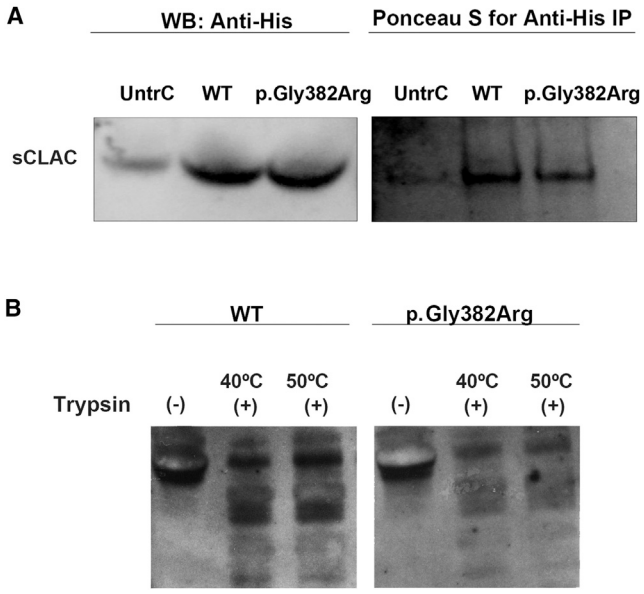

Figure 1. Effect of the p.Gly382Arg Substitution on Protein Stability

Media from HEK293 cells transfected with either wild-type (WT) or c.1144G>A containing *COL25A1* expression vector were used. (A) Left: Immunoblot analysis of secreted proteins present in culture media from untransfected control (UntrC), WT, or p.Gly382Arg-overexpressing HEK293 cells. Bands corresponding to sCLAC (~52 kDa) are enriched in WT and p.Gly382Arg-overexpressing cells but not UntrC. Right: Recombinant sCLAC was captured with anti-His-tag beads and resolved on SDS-PAGE prior to performing Ponceau S staining.
(B) Thermal stability of WT and p.Gly382Arg sCLAC. WT displayed limited proteolytic digestion at 40°C and 50°C and was completely digested at higher temperatures whereas the p.Gly382Arg protein was completely digested at all examined temperatures indicating loss of triple helix stability and folding (data for temperatures above 50°C not shown).

expression in the hippocampus and occipital lobe, moderate expression in the frontal lobe and the optic cranial nerve, and low expression in the left cerebellum were observed (Figure S3). Moreover, microarray and in situ hybridization data from Allen Brain Atlas database reported similar *COL25A1* expression in the adult human hippocampus, frontal lobe, and cerebellum cortex. Interestingly, the database documented positive expression of *COL25A1* in the adult human oculomotor nuclear complex (responsible for extraocular eye and levator palpebrae superioris muscles innervation) and in the abducens nucleus. Our cDNA data showed high *COL25A1* expression in conjunctive fibroblasts and human fetal and adult whole eye; in addition, our IHC detected moderate to strong staining in mouse eye and human eye muscle (Table S4, Figure S4). These results suggest a functional role for this gene in different regions of the brain and eye.

Glycine substitutions generally interrupt the unique collagen's repetitive pattern (Gly-Pro-X) that is required for triple helix stability; such substitutions significantly contribute to pathogenic phenotypes. Recurrence of glycine at every third position dominates proper collagen triple helix folding because it is the only amino acid with a small uncharged functional group that can center the super coiled helix without altering the helix configuration. Collagens with completely folded triple helices are typically resistant to trypsin digestion unless the helix is disrupted via increased temperatures. Peptide model of collagen, type I, alpha 1 linked to osteogenesis imperfecta (OI [MIM 166200]) showed that substituting glycine for arginine decreased the melting temperature, causing disruptive consequences.[29] Our in silico analysis with both Imutant and Pmut softwares[30,31] predicted loss of stability as a result of the p.Gly382Arg substitution. Because this change is located within a repetitive (Gly-Pro_X) stretch and involves the replacement of a glycine for arginine, we examined the sensitivity of recombinant sCLAC to trypsin digestion at different temperatures to assess the thermal stability of wild-type and p.Gly382Arg sCLAC. First we introduced the missense mutation into ready full-length ORF His/Myc *COL25A* cDNA clone (OmicsLink Expression-Ready Clones, Source BioScience) by site-directed mutagenesis (Quik Change II XL Site-Directed Mutagenesis Kit, Agilent) according to the manufacturer's protocol. After confirming the presence of the mutation by colony PCR followed by sequencing (Figure S5), cultured HEK293 cells were transfected with wild-type or mutant *COL25A1* expression vector via FuGENE 6 transfection reagent (Roche) and stable cell lines were selected in the presence of neomycin. Immunoblotting with His-tagged antibody conducted on conditioned media from transfected and untransfected HEK293 cells showed equal bands for both wild-type and the p.Gly382Arg sCLAC, indicating that both are expressed and secreted to the cell culture medium at similar levels (Figure 1A). Conditioned media collected from transfected cells stably expressing wild-type or p.Gly382Arg sCLAC were heated at 40°C–80°C for 5 min and then treated with trypsin for 2 min. The trypsin digests were inactivated and blotted with anti-His antibody. Limited digestion was observed for wild-type protein at temperatures up to 50°C whereas the p.Gly382Arg sCLAC was completely digested at all examined temperatures, suggesting loss of stability and incorrect folding, which might render the p.Gly382Arg sCLAC susceptible to proteolysis and disturb its physiological functions (Figure 1B). To further explore the effect of this substitution on sCLAC interaction with sAPP and Netrin 1 (NTN1, an APP interacting partner), sCLAC was immunoprecipitated from culture media and the precipitates and fractions of their inputs were probed against sAPP (Abcam, ab78271) and NTN1 (Abcam, ab126729). Both wild-type and p.Gly382Arg sCLAC showed similar interactions with sAPP and NTN1 (Figure S6).

Although the heterozygous c.1489G>T mutation identified in both affected and unaffected siblings DRSA1 and DRSA2 produces a truncated protein, it is plausible that the wild-type compensates for the deleterious effect of the truncated allele; therefore, the heterozygous mutation is less likely to have a pathogenic consequence on its own.

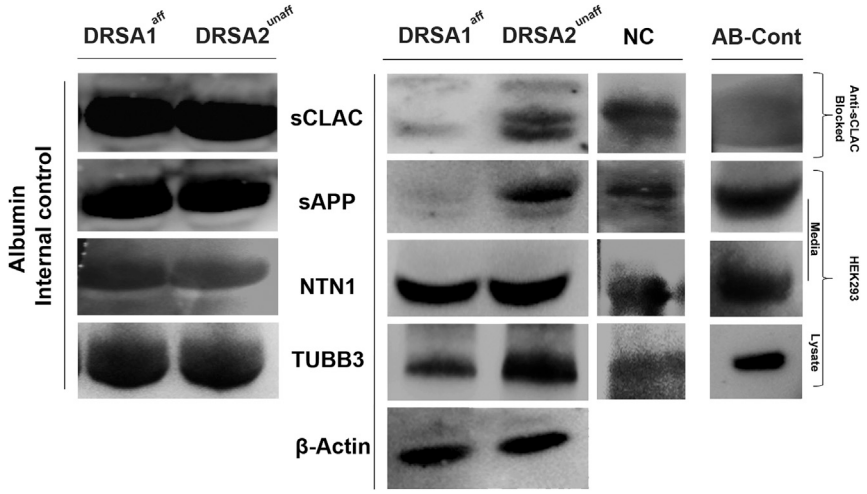

Figure 2. Assessment of sCLAC, sAPP, NTN1, and TUBB3 Levels in DRSA1

Center: Representative immunoblots for sCLAC (n = 3), sAPP (n = 2), NTN1 (n = 1), and TUBB3 (n = 3) in affected subject DRSA1 ($DRSA1^{aff}$), unaffected subject DRSA2 ($DRSA2^{unaff}$), and normal control (NC) (n = 1 for all proteins). $DRSA1^{aff}$ has diminished levels of sCLAC, low levels of sAPP, and a slightly decreased level of TUBB3 compared to $DRSA2^{unaff}$, whereas levels of NTN1 were comparable in both samples. Observed band sizes were between 52 and 76 kDa for sCLAC, sAPP, NTN1, and TUBB3. Left: Controls from either plasma or HEK293 lysate/media, referred to as antibody controls (AB-Cont), demonstrate that sAPP, NTN1, and TUBB3 band sizes correspond to those observed in other experiments. Anti-sCLAC antibody was validated by peptide block. Both β-actin (center) and albumin (right) were used as internal controls.

In DRSA1, this mutation was accompanied by an intragenic copy-number deletion that presumably contributed to the phenotype. The p.Gly497Ter truncation resulted in the loss of the C terminus COL3 and NC4 domains of COL25A1, whereas the CNV results in the loss of the entire NC2 domain including Abeta peptide/Heparin interaction site and parts of COL1 and COL2 domains (Figure S2). Intragenic copy-number deletions that remove part of the coding region can lead to truncations or a frameshift creating a premature stop codon and might result in nonsense-mediated decay (NMD) that probably diminishes the protein.[32] In line with this, our immunoblotting analysis showed diminished sCLAC in DRSA1 compared to the unaffected brother DRSA2, strongly suggesting that loss of function of both alleles is necessary for expression of the phenotype (Figure 2).

TUBB3 is a neuron-specific component of the cytoskeletal microtubules that is abundantly produced during axon guidance in the nervous system. The encoded protein is involved in the development of human ocular motor neurons and in guidance of commissural fibers and cranial nerves.[11,33] Eight distinct heterozygous missense mutations were reported in *TUBB3* in CFEOM3.[11] TUBB3 is involved in different pathways and associates with different protein partners; such associations include the direct interaction with the DCC complex that participates in proper axon guidance in the presence of functional APP and NTN1 (axon guidance tropic cue) and the direct effect on KIF21A microtubule interactions.[11,34,35]

In order to investigate the molecular consequences of the diminished sCLAC, we assessed sAPP, NTN1, and TUBB3 protein levels by immunoblot analysis in samples from DRSA1 and DRSA2. NTN1 was detected in plasma of both siblings whereas sAPP was detected with sharp band intensity only in plasma of the unaffected sibling DRSA2. TUBB3 was detected with sharp band intensity in the unaffected subject DRSA2 compared to weaker band in the affected sibling DRSA1. Both β-actin and albumin were included as internal controls (Figure 2). We also examined the level of KIF21A, which was similar in both siblings (data not shown). We hypothesize that the truncated COL25A1/sCLAC influences the signaling cascade involved in axon guidance by affecting sAPP and TUBB3 and probably other axon guidance molecules during development. This hypothesis is supported by the compromised sAPP and TUBB3 levels observed in this single case subject and the sustained NTN1 interaction with sCLAC detected by immunoprecipitation assay.

Col25a1 knockout mice exhibited loss of motor axon elongation and branching in the muscles, which resulted in axon degeneration. This effect leads to death due to respiratory failure, which highlights the regulatory role for COL25A1 in intramuscular innervation during development.[36] All our case subjects with mutations in *COL25A1* showed variable ophthalmological clinical presentation with no other systemic defects. Two of the affected individuals from family A (II.1 and II.2) with mutations in *COL25A1* were diagnosed with levator palpebrae muscle dysinnervation (congenital ptosis) of one or both orbits. The levator palpebrae muscle is normally innervated by the oculomotor nerve (cranial nerve III).[2] The third affected member of family A (II.3) was diagnosed with dysinnervation to the lateral and/or medial rectus muscles of both eyes. The medial rectus muscle is normally innervated by inferior division of the oculomotor nerve and the lateral rectus muscle is normally innervated by the abducens nerve (cranial nerve VI).[1] Abnormalities of guidance and survival of the cranial nerves underlie different CCDD phenotypes.

Taken together, we identified *COL25A1* mutations as a cause of autosomal-recessive CCDD. Our molecular characterization of the protein and the transcript demonstrated their presence in human eye muscle and in fetal and adult brain, respectively. Further assessment of mutations in this

gene suggests that a defective protein interferes with molecules involved in axon guidance and might result in abnormal cytoskeletal microtubule dynamics and atypical ocular motor neuron development. Further investigations are necessary to elucidate the possible regulatory effect of functional COL25A1 on the levels of APP, TUBB3, and other proteins, including KIF21A, relevant to ocular motor neuron development.

Supplemental Data

Supplemental Data include six figures and four tables and can be found with this article online at http://dx.doi.org/10.1016/j.ajhg.2014.11.006.

Acknowledgments

The authors would like to thank Dorota Moniez and the sequencing core facility members for their help in DNA sequencing and Salma Wakil and the genotyping core facility members for their help in genotyping. We would like to thank Bashayer AlMubarak for her valuable input. This work was approved and funded by KFSHRC (RAC # 2080020) and KKESH (0424-P).

Received: July 29, 2014
Accepted: November 11, 2014
Published: December 11, 2014

Web Resources

The URLs for data presented herein are as follows:

Allen Brain Atlas, http://www.brain-map.org/
dbSNP, http://www.ncbi.nlm.nih.gov/projects/SNP/
Ensembl Genome Browser, http://www.ensembl.org/index.html
GenBank, http://www.ncbi.nlm.nih.gov/genbank/
GeneCards, http://www.genecards.org
I-Mutant, http://folding.biofold.org/i-mutant/i-mutant2.0.html
MOPED, https://www.proteinspire.org/MOPED/mopedviews/proteinExpressionDatabase.jsf
Online Mendelian Inheritance in Man (OMIM), http://www.omim.org/
PaxDb, http://pax-db.org/#!home
Pmut, http://mmb.pcb.ub.es/PMut
RefSeq, http://www.ncbi.nlm.nih.gov/RefSeq
UCSC Genome Browser, http://genome.ucsc.edu

Accession Numbers

Submitter SNP numbers from dbSNP for variants identified in this study are ss1388022660, ss1388022661, ss1388022662, ss1388022663, ss1388022664, ss1388022665, ss1388022666, ss1388022667, ss1388022668, ss1388022669, ss1388022670, ss1388022671, ss1388022672, and ss1388022673.

References

1. Gutowski, N.J., Bosley, T.M., and Engle, E.C. (2003). 110th ENMC International Workshop: the congenital cranial dysinnervation disorders (CCDDs). Naarden, The Netherlands, 25-27 October, 2002. Neuromuscul. Disord. *13*, 573–578.
2. Engle, E.C., Goumnerov, B.C., McKeown, C.A., Schatz, M., Johns, D.R., Porter, J.D., and Beggs, A.H. (1997). Oculomotor nerve and muscle abnormalities in congenital fibrosis of the extraocular muscles. Ann. Neurol. *41*, 314–325.
3. Yamada, K., Andrews, C., Chan, W.M., McKeown, C.A., Magli, A., de Berardinis, T., Loewenstein, A., Lazar, M., O'Keefe, M., Letson, R., et al. (2003). Heterozygous mutations of the kinesin KIF21A in congenital fibrosis of the extraocular muscles type 1 (CFEOM1). Nat. Genet. *35*, 318–321.
4. Doherty, E.J., Macy, M.E., Wang, S.M., Dykeman, C.P., Melanson, M.T., and Engle, E.C. (1999). CFEOM3: a new extraocular congenital fibrosis syndrome that maps to 16q24.2-q24.3. Invest. Ophthalmol. Vis. Sci. *40*, 1687–1694.
5. Tischfield, M.A., Bosley, T.M., Salih, M.A., Alorainy, I.A., Sener, E.C., Nester, M.J., Oystreck, D.T., Chan, W.M., Andrews, C., Erickson, R.P., and Engle, E.C. (2005). Homozygous HOXA1 mutations disrupt human brainstem, inner ear, cardiovascular and cognitive development. Nat. Genet. *37*, 1035–1037.
6. Bosley, T.M., Salih, M.A., Jen, J.C., Lin, D.D., Oystreck, D., Abu-Amero, K.K., MacDonald, D.B., al Zayed, Z., al Dhalaan, H., Kansu, T., et al. (2005). Neurologic features of horizontal gaze palsy and progressive scoliosis with mutations in ROBO3. Neurology *64*, 1196–1203.
7. Chung, M., Stout, J.T., and Borchert, M.S. (2000). Clinical diversity of hereditary Duane's retraction syndrome. Ophthalmology *107*, 500–503.
8. Khan, A.O., Shinwari, J., Omar, A., Al-Sharif, L., Khalil, D.S., Alanazi, M., Al-Amri, A., and Al Tassan, N. (2011). Lack of KIF21A mutations in congenital fibrosis of the extraocular muscles type I patients from consanguineous Saudi Arabian families. Mol. Vis. *17*, 218–224.
9. Nakano, M., Yamada, K., Fain, J., Sener, E.C., Selleck, C.J., Awad, A.H., Zwaan, J., Mullaney, P.B., Bosley, T.M., and Engle, E.C. (2001). Homozygous mutations in ARIX(PHOX2A) result in congenital fibrosis of the extraocular muscles type 2. Nat. Genet. *29*, 315–320.
10. Khan, A.O., Almutlaq, M., Oystreck, D.T., Engle, E.C., Abu-Amero, K., and Bosley, T. (2014). Retinal dysfunction in patients with congenital fibrosis of the extraocular muscles type 2. Ophthalmic Genet., 1–7.
11. Tischfield, M.A., Baris, H.N., Wu, C., Rudolph, G., Van Maldergem, L., He, W., Chan, W.M., Andrews, C., Demer, J.L., Robertson, R.L., et al. (2010). Human TUBB3 mutations perturb microtubule dynamics, kinesin interactions, and axon guidance. Cell *140*, 74–87.
12. Yamada, K., Chan, W.M., Andrews, C., Bosley, T.M., Sener, E.C., Zwaan, J.T., Mullaney, P.B., Oztürk, B.T., Akarsu, A.N., Sabol, L.J., et al. (2004). Identification of KIF21A mutations as a rare cause of congenital fibrosis of the extraocular muscles type 3 (CFEOM3). Invest. Ophthalmol. Vis. Sci. *45*, 2218–2223.
13. Hotchkiss, M.G., Miller, N.R., Clark, A.W., and Green, W.R. (1980). Bilateral Duane's retraction syndrome. A clinical-pathologic case report. Arch. Ophthalmol. *98*, 870–874.
14. Miyake, N., Chilton, J., Psatha, M., Cheng, L., Andrews, C., Chan, W.M., Law, K., Crosier, M., Lindsay, S., Cheung, M., et al. (2008). Human CHN1 mutations hyperactivate alpha2-chimaerin and cause Duane's retraction syndrome. Science *321*, 839–843.
15. Jen, J.C., Chan, W.M., Bosley, T.M., Wan, J., Carr, J.R., Rüb, U., Shattuck, D., Salamon, G., Kudo, L.C., Ou, J., et al. (2004). Mutations in a human ROBO gene disrupt hindbrain axon

pathway crossing and morphogenesis. Science *304*, 1509–1513.
16. Khan, A.O., Khalil, D.S., Al-Sharif, L.J., and Al-Tassan, N.A. (2009). Mutations in KIF21A and PHOX2A are absent in 16 patients with congenital vertical incomitant strabismus. Ophthalmic Genet. *30*, 206–207.
17. Lindner, T.H., and Hoffmann, K. (2005). easyLINKAGE: a PERL script for easy and automated two-/multi-point linkage analyses. Bioinformatics *21*, 405–407.
18. Adie, E.A., Adams, R.R., Evans, K.L., Porteous, D.J., and Pickard, B.S. (2005). Speeding disease gene discovery by sequence based candidate prioritization. BMC Bioinformatics *6*, 55.
19. Yang, M.M., Ho, M., Lau, H.H., Tam, P.O., Young, A.L., Pang, C.P., Yip, W.W., and Chen, L. (2013). Diversified clinical presentations associated with a novel sal-like 4 gene mutation in a Chinese pedigree with Duane retraction syndrome. Mol. Vis. *19*, 986–994.
20. Engle, E.C., Castro, A.E., Macy, M.E., Knoll, J.H., and Beggs, A.H. (1997). A gene for isolated congenital ptosis maps to a 3-cM region within 1p32-p34.1. Am. J. Hum. Genet. *60*, 1150–1157.
21. McMullan, T.W., Crolla, J.A., Gregory, S.G., Carter, N.P., Cooper, R.A., Howell, G.R., and Robinson, D.O. (2002). A candidate gene for congenital bilateral isolated ptosis identified by molecular analysis of a de novo balanced translocation. Hum. Genet. *110*, 244–250.
22. Cederquist, G.Y., Luchniak, A., Tischfield, M.A., Peeva, M., Song, Y., Menezes, M.P., Chan, W.M., Andrews, C., Chew, S., Jamieson, R.V., et al. (2012). An inherited TUBB2B mutation alters a kinesin-binding site and causes polymicrogyria, CFEOM and axon dysinnervation. Hum. Mol. Genet. *21*, 5484–5499.
23. MacKinnon, S., Oystreck, D.T., Andrews, C., Chan, W.M., Hunter, D.G., and Engle, E.C. (2014). Diagnostic distinctions and genetic analysis of patients diagnosed with moebius syndrome. Ophthalmology *121*, 1461–1468.
24. Hashimoto, T., Wakabayashi, T., Watanabe, A., Kowa, H., Hosoda, R., Nakamura, A., Kanazawa, I., Arai, T., Takio, K., Mann, D.M., and Iwatsubo, T. (2002). CLAC: a novel Alzheimer amyloid plaque component derived from a transmembrane precursor, CLAC-P/collagen type XXV. EMBO J. *21*, 1524–1534.
25. Osada, Y., Hashimoto, T., Nishimura, A., Matsuo, Y., Wakabayashi, T., and Iwatsubo, T. (2005). CLAC binds to amyloid beta peptides through the positively charged amino acid cluster within the collagenous domain 1 and inhibits formation of amyloid fibrils. J. Biol. Chem. *280*, 8596–8605.
26. Kakuyama, H., Söderberg, L., Horigome, K., Winblad, B., Dahlqvist, C., Näslund, J., and Tjernberg, L.O. (2005). CLAC binds to aggregated Abeta and Abeta fragments, and attenuates fibril elongation. Biochemistry *44*, 15602–15609.
27. Tyler, S.J., Dawbarn, D., Wilcock, G.K., and Allen, S.J. (2002). alpha- and beta-secretase: profound changes in Alzheimer's disease. Biochem. Biophys. Res. Commun. *299*, 373–376.
28. Parmar, A.S., Nunes, A.M., Baum, J., and Brodsky, B. (2012). A peptide study of the relationship between the collagen triple-helix and amyloid. Biopolymers *97*, 795–806.
29. Beck, K., Chan, V.C., Shenoy, N., Kirkpatrick, A., Ramshaw, J.A., and Brodsky, B. (2000). Destabilization of osteogenesis imperfecta collagen-like model peptides correlates with the identity of the residue replacing glycine. Proc. Natl. Acad. Sci. USA *97*, 4273–4278.
30. Capriotti, E., Fariselli, P., and Casadio, R. (2005). I-Mutant2.0: predicting stability changes upon mutation from the protein sequence or structure. Nucleic Acids Res. *33*, W306–W310.
31. Ferrer-Costa, C., Gelpí, J.L., Zamakola, L., Parraga, I., de la Cruz, X., and Orozco, M. (2005). PMUT: a web-based tool for the annotation of pathological mutations on proteins. Bioinformatics *21*, 3176–3178.
32. Boone, P.M., Bacino, C.A., Shaw, C.A., Eng, P.A., Hixson, P.M., Pursley, A.N., Kang, S.H., Yang, Y., Wiszniewska, J., Nowakowska, B.A., et al. (2010). Detection of clinically relevant exonic copy-number changes by array CGH. Hum. Mutat. *31*, 1326–1342.
33. Katsetos, C.D., Legido, A., Perentes, E., and Mörk, S.J. (2003). Class III beta-tubulin isotype: a key cytoskeletal protein at the crossroads of developmental neurobiology and tumor neuropathology. J. Child Neurol. *18*, 851–866, discussion 867.
34. Qu, C., Dwyer, T., Shao, Q., Yang, T., Huang, H., and Liu, G. (2013). Direct binding of TUBB3 with DCC couples netrin-1 signaling to intracellular microtubule dynamics in axon outgrowth and guidance. J. Cell Sci. *126*, 3070–3081.
35. Rama, N., Goldschneider, D., Corset, V., Lambert, J., Pays, L., and Mehlen, P. (2012). Amyloid precursor protein regulates netrin-1-mediated commissural axon outgrowth. J. Biol. Chem. *287*, 30014–30023.
36. Tanaka, T., Wakabayashi, T., Oizumi, H., Nishio, S., Sato, T., Harada, A., Fujii, D., Matsuo, Y., Hashimoto, T., and Iwatsubo, T. (2014). CLAC-P/collagen type XXV is required for the intramuscular innervation of motoneurons during neuromuscular development. J. Neurosci. *34*, 1370–1379.